Data assimilation of sea-ice motion vectors: sensitivity to the parameterization of sea-ice strength

Mingrui DAI,* Todd E. ARBETTER,† Walter N. MEIER

National Snow and Ice Data Center/World Data Center for Glaciology, University of Colorado, Boulder, CO 80309-0449, USA
E-mail: mingdai@nsidc.org

ABSTRACT. Data assimilation techniques are one method by which to improve the quality of model simulations of sea ice. The availability of daily gridded fields of sea-ice motion makes this field one that can be readily assimilated. These fields are generally of higher resolution than forcing values such as atmospheric wind which are used to drive the model, and on any given day may depict ice circulation that is dramatically different than what the model solution represents. Typically, a blending method such as optimal interpolation (OI) is used and corrections are applied to the initial modeled velocity field such that the new solution corresponds better with actual observations. However, care must be taken in such a technique, as the corrections are not applied directly to the model physics, and the underlying physical assumptions in the ice dynamics may be violated. Previous studies have shown that improvements in the ice-motion solution come at the cost of the quality of other modeled fields. The strength parameterization in sea-ice models controls the ice velocity in the model, and is obtained in part by comparison with observed motions. Here we investigate the sensitivity of the sea-ice model to variations in the strength parameterization, and determine the effect of using data assimilation to impose observed velocities. We find that the alternation of the frictional loss parameter has limited effect on model performance. Rather, it is the assimilated data that overwhelm and degrade the solution, bringing into question whether underlying physical assumptions in the model may be compromised.

INTRODUCTION

Data assimilation techniques are one method by which to improve the quality of model simulations of sea ice. The need for data assimilation arises from the facts that, first, physical models are far from perfect and data assimilation can compensate model errors; and second, assimilation technique provides the mechanism for extracting useful information from noisy data, while the model provides the mechanism for constraining data and carrying information forward. The techniques used for assimilation can be divided into two broad categories: sequential and model-trajectory methods. Direct insertion, nudging, optimal interpolation (OI) and Kalman filter are examples of sequential methods. Because this paper focuses on sequential methods, especially OI, model-trajectory methods are not discussed here. For ice data, Maslanik and Maybee (1994) assimilated Advanced Very High Resolution Radiometer (AVHRR)-derived ice motion into a dynamic–thermodynamic ice model using direct insertion; Thomas and others (1996) assimilated Special Sensor Microwave Radiometer (SSMR)-derived ice concentration into an ice-thickness distribution model using a Kalman smoother; and Meier and others (2000), Arbetter and others (2002) and Zhang and others (2003) assimilated Special Sensor Microwave/Imager (SSM/I)-derived ice motion using OI. Lindsay and Zhang (2005) assimilated ice motion and ice concentration using OI and nudging.

Previous studies have shown that assimilation of observed ice motion significantly improves the calculation of ice motion (Meier and others, 2000; Zhang and others, 2003). However, it has mixed effects on the quality of other modeled fields. Zhang and others (2003) showed that assimilation of ice motion improved the model performance on ice thickness. They believe that the strengthened spatial gradients of velocity after assimilation are likely to be the reason. Arbetter and others (2002) showed excessive summer ice melting after assimilating observed ice motion. A significant difference between the Arbetter and others (2002) approach and the previous studies is that Arbetter and others assimilated motions through the summer melt season, while the other studies assimilated motions only during fall through spring. Arbetter and others concluded that the increased open-water creation through enhanced divergence provides a mechanism during summer to accelerate the ice melting. Their results implied that modeled ice-motion fields (without assimilation) differ from the observed ice-motion field in such a way as to be significant enough to violate the underlying physical assumptions of the model.

In this study, we first try to verify the difference between modeled and observed ice-motion fields. Then we investigate the model sensitivities to some physical processes or parameterizations to provide clues for further fine-tuning of the model. The strength parameterization in sea-ice models controls the ice velocity in the model (Flato and Hibler, 1995) and is obtained in part by comparing modeled with observed ice motions. Thus, it is logical for us to study the sensitivity of the sea-ice model to variations in the strength parameterization.

MODEL, FORCING DATA AND DATA ASSIMILATION

The sea-ice model used here is similar to that described by Flato and Hibler (1995). It is implemented on a 166×161

*Present address: Canadian Ice Service, Meteorological Service of Canada, Environment Canada, 373 Sussex Drive, Ottawa, Ontarioa K1A 0H3, Canada.
†Present addresss: British Antarctic Survey, Natural Environment Research Council, Madingley Road, Cambridge CB3 0ET, UK.

https://doi.org/10.3189/172756406781811187 Published online by Cambridge University Press

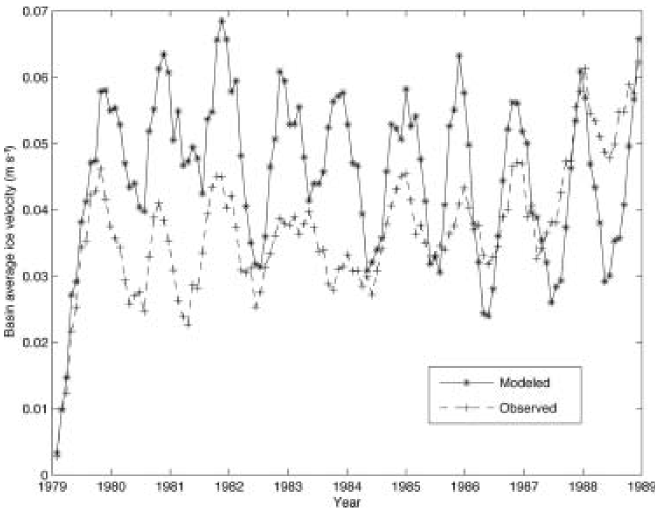

Fig. 1. Modeled (case 1) and observed basin average ice speed.

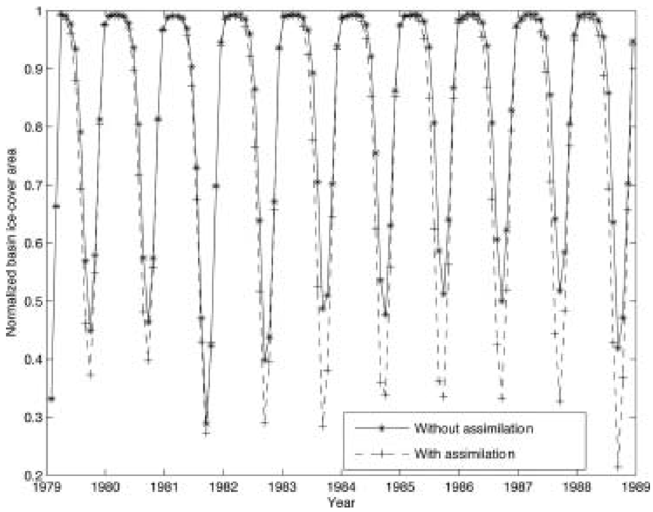

Fig. 2. The effects of assimilation ($C_f = 17$).

Cartesian grid derived from the Equal-Area Scalable Earth (EASE) projection (Armstrong and others, 1997) with a grid size of 25 km. Each gridcell contains 12 ice categories, each category having a fixed mean thickness (Thorndike and others, 1975; Hibler, 1980). A viscous–plastic rheology (Hibler, 1979) is used here, with the alternate-direction implicit solver employed (Zhang and Rothrock, 2000). Ridging and vertical redistribution of the sea ice within each gridcell are determined using formulations for ice strength (Rothrock, 1975) and ice divergence within each cell (Thorndike and others, 1975; Hibler, 1980).

The ice-strength parameterization reads

$$p = C_f C_p \int_0^\infty (\omega_r + \omega_u) h^2 \, dh, \tag{1}$$

where $C_p = 1/2(\rho_i/\rho_w)g(\rho_w - \rho_i)$ is a constant in which ρ_i and ρ_w are the densities of ice and water, respectively, and g is the acceleration due to gravity. ω_r and ω_u are so-called ridging modes, which describe the transfer of thin ice into a distribution of thicker, ridged ice (Rothrock, 1975; Thorndike and others, 1975; Hibler, 1980; Flato and Hibler, 1995). h is ice thickness, and frictional parameter C_f is defined as the ratio of total energy loss to potential energy change and is the parameter that controls the compressive strength of the ice cover. C_f is a tunable parameter and is determined by comparing the computed and observed ice drift. $C_f = 2$ is used by Hibler (1980), while $C_f = 17$ is used by Flato and Hibler (1995) in their baseline simulation.

The forcing data used are the US National Centers for Environmental Prediction (NCEP) re-analysis (Kalnay and others, 1996), and the observed ice motion used in this study is the Polar Pathfinder daily 25 km EASE-Grid sea-ice motion vectors (C. Fowler, http://nsidc.org/data/nsidc-0116.html). Daily ice-motion vectors are computed from AVHRR, Scanning Multichannel Microwave Radiometer (SMMR) and SSM/I using a maximum cross-correlation technique (Emery and others, 1991). Daily ice motions are also calculated from International Arctic Buoy Programme (IABP) (Rigor and Colony, 1995) buoy data. Daily gridded fields combine data from all sensors (for a detailed technical description of the ice-motion data, see C. Fowler, http://nsidc.org/data/nsidc-0116.html). An optimum interpolation method is used to assimilate this daily gridded ice motion into the ice model (Meier and others 2000; Meier and Maslanik, 2001).

Table 1. Test cases

Case No.	Assimilation	C_f
1	No	17
2	No	2
3	No	34
4	Yes	17
5	Yes	2

RESULTS

We ran a total of five cases, as summarized in Table 1, to test the sensitivities of the model to variations in the strength parameterization and the effects of data assimilation.

We first compare the modeled ice motions with the observed ice motions (experiments 1–3). We use the basin average ice speed as the baseline of comparison, where the Arctic basin is defined following Gloersen and others (1992). The modeled (without assimilation) basin average ice speed is defined as the spatial average of ice speed at any gridcell where ice concentration is >15%. The observed basin average ice speed is defined as the spatial average of ice speed from the daily gridded ice-motion dataset mentioned in the previous section. As shown in Figure 1, we can see that the modeled ice speed is significantly different from the observed ice speed. The 10 year mean of the modeled basin average ice speed is 4.66 cm s^{-1}, while the 10 year mean of the observed basin average ice speed is 3.82 cm s^{-1}. The seasonal fluctuation of the modeled ice speed is also greater than that of the observed ice speed.

Experiments 4 and 5 assimilate the daily observed ice velocities into the model solution. As expected, assimilation of such different ice-motion data into the ice model greatly impacts the model behavior. In Figure 2, we show the normalized basin ice-cover area for cases with and without assimilation of ice motion. Here the ice-cover area is normalized by the basin area. In winter, the basin is totally

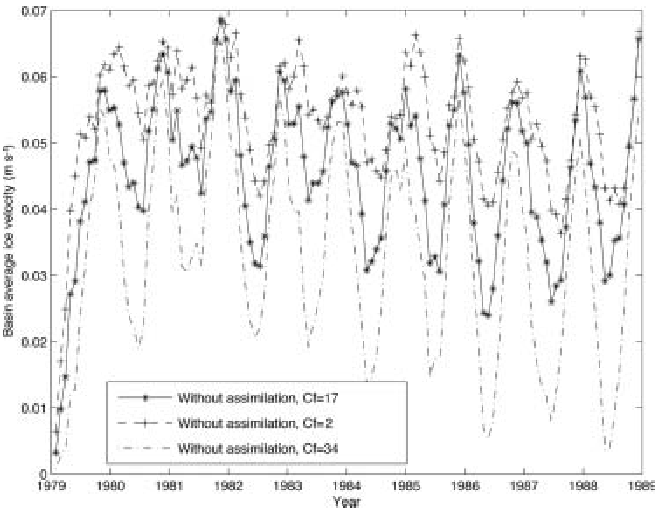

Fig. 3. Effects of C_f on basin average ice speed (without assimilation).

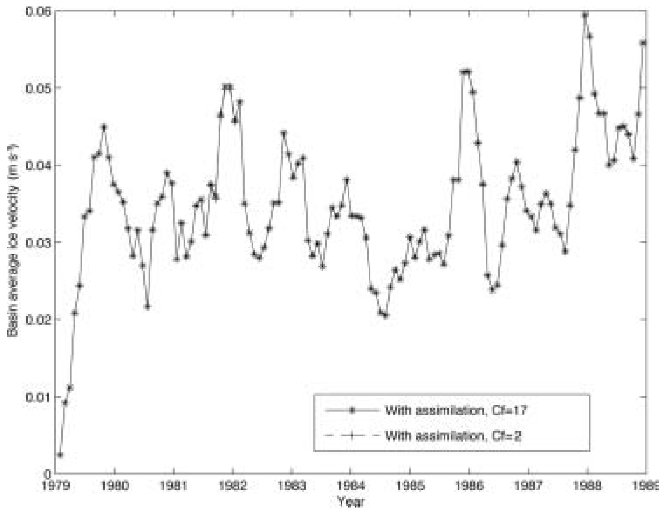

Fig. 5. Effects of C_f on basin average ice speed (with assimilation). Note that the effects are very small and the two curves almost overlap each other.

covered by ice; hence the normalized basin ice-cover area approaches unity. From Figure 2 we can see that the modeled (without assimilation) summer ice-cover area is around 50% of the winter ice-cover area, which agrees with the satellite observations (Gloersen and Campbell, 1991). The assimilation reduces the summer ice-cover area by up to 40%.

Variations of frictional loss parameter C_f significantly change the ice speed and the ice-cover area in cases without assimilation, as shown in Figures 3 and 4. However, C_f has limited effects on the ice drift and ice-cover area in cases with assimilation, as shown in Figures 5 and 6. It seems that the assimilation has an overwhelming effect, constraining the solution to observations.

CONCLUSION AND DISCUSSION

In this study, we investigate the model sensitivities to strength parameterization to provide clues for further improvements to the model. Assimilation of observed ice motion constrains the model solution to closely resemble observations, but causes excessive summer ice retreat. Efforts to adjust the model by altering the frictional loss parameter have limited effects in the assimilated cases, because the assimilation of observed ice motion essentially bypasses the model dynamics.

In reality, sea ice is composed of a number of discrete floes with sizes ranging from a few meters to tens of kilometers or more. These floes grow thermodynamically and are deformed due to wind and water stresses, which cause the floes to break apart (divergence) or form rubble fields and pressure ridges (convergence). It is essential to recognize that all models are at some level a mathematical parameterization of these processes. The viscous–plastic rheology (Hibler 1979, 1980) contains an underlying assumption that the sea ice in the Arctic can be described as continuous fluid.

While others have successfully run continuum models at resolutions finer than the 25 km used here, to our knowledge they have not incorporated high-resolution ice-motion data

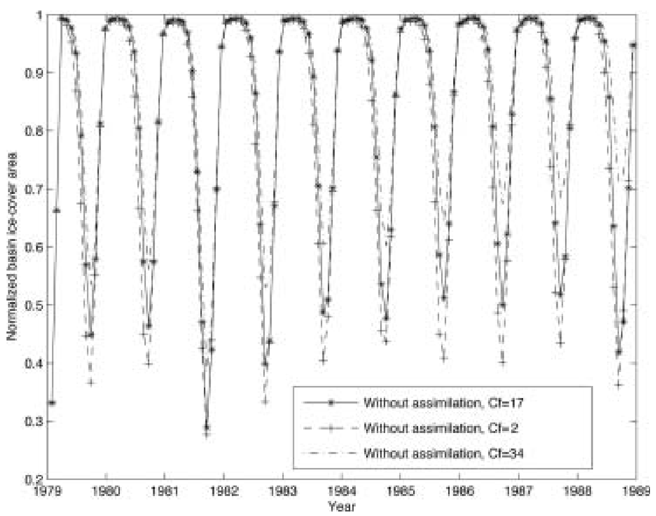

Fig. 4. Effects of C_f on basin ice-cover area (without assimilation).

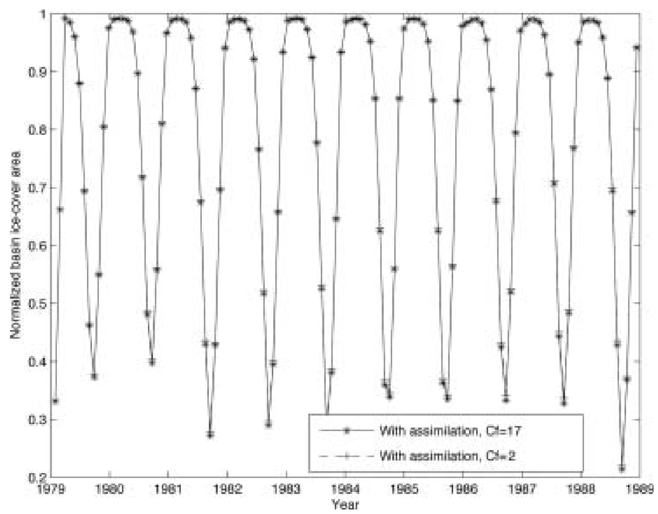

Fig. 6. Effects of C_f on basin ice-cover area (with assimilation). Note that the effects are very small and two curves almost overlap each other.

https://doi.org/10.3189/172756406781811187 Published online by Cambridge University Press

(including summertime observations) on a basin-wide scale over several annual cycles. The observed ice-motion vectors show discontinuities which likely indicate where floes are divergent. When these motions are assimilated into the model, the solution does show divergence in the same location as observed; this results in much of the ice volume being advected out of the gridcell. However, in summer there exists no mechanism to grow new ice. Lateral melting in the model is accelerated with the increased open water, and much of the sea ice is lost by the end of the summer.

It is not enough to assume that the summertime ice motions are problematic and should be ignored. Rather, the problems indicate that an observed feature of sea ice is not reproduced well by the model, and in this case the excessive ice divergences introduced may violate the model's physical assumptions (although not necessarily or exclusively the dynamic component). A thorough parameter estimation, including dynamic and thermodynamic parts of the model, is necessary to improve model behavior within the constraints of the observed ice motions. Hargreaves and others (2004) and Annan and others (2005) simultaneously estimated 12 parameters in an intermediate-complexity coupled atmosphere and ocean global climate model (AOGCM) using an ensemble Kalman filter technique with only 50 runs. Their works suggest a future direction to further improve the ice model.

ACKNOWLEDGEMENTS

This work was supported by NASA contract NAG5-10556 and a University Corporation for Atmospheric Research (UCAR) Visiting Scientist Fellowship.

REFERENCES

Annan, J.P., J.C. Hargreaves, N.R. Edwards and R. Marsh. 2005. Parameter estimation in an intermediate complexity earth system model using an ensemble Kalman filter. *Ocean Model.,* **8**(1–2), 135–154.

Arbetter, T.E., A.H. Lynch, J.A. Maslanik and W.N. Meier. 2002. Effects of data assimilation of ice motion in a basin-scale sea ice model. *In* Squire, V.A. and P. Langhorne, *eds. Ice in the Environment, Proceedings of the 16th IAHR International Symposium on Ice, 2–6 December 2002, Dunedin, New Zealand, Vol. 3.* Dunedin, International Association of Hydraulic Engineering and Research, 186–193.

Armstrong, R.L., M.J. Brodzik and A. Varani. 1997. The NSIDC EASE-Grid: addressing the need for a common, flexible, mapping and gridding scheme. *Earth Syst. Monitor,* **7**(4), 6–7, 14.

Bitz, C.M. and W.H. Lipscomb. 1999. An energy-conserving thermodynamic model of sea ice. *J. Geophys. Res.,* **104**(C7), 15,669–15,677.

Emery, W.J., C.W. Fowler, J. Hawkins and R.H. Preller. 1991. Fram Strait satellite image-derived ice motions. *J. Geophys. Res.,* **96**(C3), 4751–4768. (*Correction*: **96**(C5), 1991, 8917–8920.)

Flato, G.M. and W.D. Hibler, III. 1995. Ridging and strength in modeling the thickness distribution of Arctic sea ice. *J. Geophys. Res.,* **100**(C9), 18,611–18,626.

Gloersen, P. and W.J. Campbell. 1991. Recent variations in Arctic and Antarctic sea-ice covers. *Nature,* **352**(6330), 33–36.

Gloersen, P., W.J. Campbell, D.J. Cavalieri, J.C. Comiso, C.L. Parkinson and H.J. Zwally. 1992. *Arctic and Antarctic sea ice, 1978–1987: satellite passive-microwave observations and analysis.* Washington, DC, National Aeronautics and Space Administration. (NASA SP-511.)

Hargreaves, J.C., J.P. Annan, N.R. Edwards and R. Marsh. 2004. An efficient climate forecasting method using an intermediate complexity Earth System Model and the ensemble Kalman filter. *Climate Dyn.,* **23**(7–8), 745–760.

Hibler, W.D., III. 1979. A dynamic thermodynamic sea ice model. *J. Phys. Oceanogr.,* **9**(7), 815–846.

Hibler, W.D., III. 1980. Modeling a variable thickness sea ice cover. *Mon. Weather Rev.,* **108**(12), 1943–1973.

Kalnay, E. *and 21 others.* 1996. The NCEP/NCAR 40-year reanalysis project. *Bull. Am. Meteorol. Soc.,* **77**(3), 437–471.

Lindsay, R.W. and J. Zhang. 2005. Assimilation of ice concentration in an ice–ocean model. *J. Atmos. Ocean Tech.,* **23**(5), 742–749.

Meier, W.N. and J.A. Maslanik. 2001. Synoptic-scale ice-motion case-studies using assimilated motion fields. *Ann. Glaciol.,* **33**, 145–150.

Meier, W.N., J.A. Maslanik and C.W. Fowler. 2000. Error analysis and assimilation of remotely sensed ice motion within an Arctic sea ice model. *J. Geophys. Res.,* **105**(C2), 3339–3356.

Rigor, I. and R.L. Colony. 1995. *International Arctic Buoy Program data report: 1 January 1993–31 December 1993.* Seattle, WA, University of Washington. Applied Physics Laboratory. (Tech. Memo. APL-UW TM 4-95.)

Rothrock, D.A. 1975. The energetics of the plastic deformation of pack ice by ridging. *J. Geophys. Res.,* **80**(33), 4514–4519.

Thomas, D., S. Martin, D. Rothrock and M. Steele. 1996. Assimilating satellite concentration data into an Arctic sea ice mass balance model, 1979–1985. *J. Geophys. Res.,* **101**(C9), 20,849–20,868.

Thorndike, A.S., D.A. Rothrock, G.A. Maykut and R. Colony. 1975. The thickness distribution of sea ice. *J. Geophys. Res.,* **80**(33), 4501–4513.

Zhang, J. and D. Rothrock. 2000. Modeling Arctic sea ice with an efficient plastic solution. *J. Geophys. Res.,* **105**(C2), 3325–3338.

Zhang, J., D.A. Rothrock, R.W. Lindsay and Y. Yu. 2003. Assimilation of ice motion observations and comparisons with submarine ice thickness data. *J. Geophys. Res.,* **108**(C6), 3170. (10.1029/2001JC002041.)